

Composite, Grid-Stiffened Panel Design for Post Buckling Using Hypersizer®

Craig Collier* and Phil Yarrington

<http://hypersizer.com/>

info@hypersizer.com

Collier Research Corporation

Hampton, Virginia

Barry Van West

The Boeing Company

Seattle, Washington

ABSTRACT

Due to weight and cost goals, a grid-stiffened panel concept is being used for redesign of a structural component on the Minotaur OSP space launch vehicle. By designing the structural panels to carry operational loads past the point of initial buckling (local post-buckling), the resulting grid stiffened panel concept is lighter and 30% less costly to manufacture than other design candidates such as the existing honeycomb sandwich panel concept flown today. During June 2001 in Seattle, Boeing performed a structural certification experiment of a composite, grid stiffened, cylindrical panel loaded in axial compression. Pretest predictions were made for linear elastic (bifurcation) buckling, and non-linear post buckling. The tools used for pretest analysis were HyperSizer®, and the FEM based tools MSC/NASTRAN™ and STAGS™. Local buckling of the facesheet triangular shaped skin pocket occurred at a load of around 230 (lb/in). The test panel was able to sustain considerable additional loading, with post buckling failure occurring at 1320 (lb/in). The HyperSizer post buckling pretest prediction was 1300 (lb/in), the STAGS pretest prediction was 1250 (lb/in), and the MSC/NASTRAN pretest prediction ranged from 1425 to 2000 (lb/in). HyperSizer's implementation of local post buckling based on an effective width approach is presented.

1. INTRODUCTION

There is an industry need to analyze and optimize stiffened panels in a computationally efficient practical manner for hundreds of load cases while still maintaining reliable accuracy. The commercial HyperSizer software was developed for this purpose. HyperSizer is not another FEA program, but rather a structural analysis and sizing optimization package. It will automatically import FEA computed internal loads, perform the analysis and optimization, and then update

the FEM's stiffness properties to reflect the current design. This primary mode of operation is for performing system level sizing. In addition, as in the case of the presented experimental test that follows, the loads and boundary conditions can be entered directly into HyperSizer without the need for FEA.

1.1 Application

Some various shaped stiffening members commonly used for panel structural concepts are "T", "Z", "J", "I", blade, and hat. The stiffening member provides the benefit of added load-carrying capability with a relatively small additional weight penalty. Most stiffened panel designs provide high bending stiffness in only one direction. The principal alternative to stiffened panel designs are sandwich designs, such as honeycomb. However, unidirectionally designed panels cost less and are easier to inspect and most applications do not require high bending stiffness in both directions.

In the aerospace industry stiffened panels have and continue to be used for external surfaces of aircraft and space launch vehicles. Thermal forces and moments induced from temperature gradients are smaller for stiffened panels than they are for sandwich type panels. These reduced thermal loads make them efficient as hot structure for space applications and launch vehicles.



Fig. 1, A grid-stiffened panel with longitudinal and angle ribs.

However there are many applications for grid-stiffened structures that have stiffeners running in two, three, and four different directions, Fig. 1. Their use in the past has mostly been with isotropic, machined metals [1]. Only recently has the industry developed methods to economically fabricate grid stiffened panel concepts with fiber-reinforced advanced composite material [2]. One solution uses multiple tooling materials which leads to the name "Hybrid Tooling", Fig. 2. The combination of materials allows for precise control of lateral rib compaction, while maintaining process controllability. The Hybrid Tooling concept, developed by the Air Force Research Laboratory, Space Vehicles Directorate is proven to be compatible with filament winding and expected to be compatible with fiber placement. In their studies, the traditional equilateral

* Senior member AIAA

triangle pattern that produces isotropic-like behavior, and leads to the name isogrid, has been abandoned in favor of stiffener patterns optimized to specified loading situations.

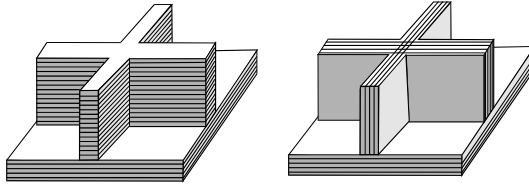


Fig. 2, A Hybrid and non-hybrid layup.

1.2 Software

To address these emerging structural concepts, the grid-stiffened family of panels was added to the HyperSizer structural analysis and sizing optimization software, Fig. 3. Isotropic, equivalent orthotropic and general laminated composites are fully supported for the IsoGrid, OrthoGrid, XGrid, YGrid, BiGrid, and GeneralGrid rib-stiffened panel concepts. Sandwich BiGrid, IsoGrid, and OrthoGrid concepts are also included. The implementation is quite general. For sizing optimization, the longitudinal (0), transverse (90), and angle (theta) ribs can all have different thicknesses, spacings, and heights. The angle rib can have any angle. The facesheets and webs can be different materials, laminates, or layups.

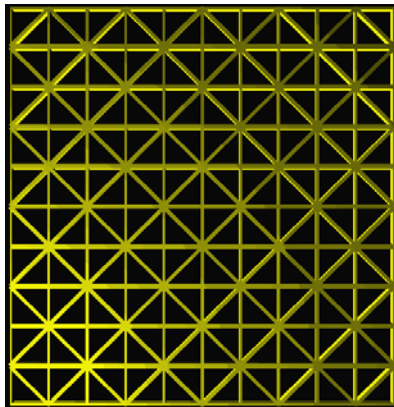


Fig. 3, HyperSizer graphic display of an optimum grid stiffened pattern, rib spacing, thickness, and height.

This generality, accuracy of analysis, and quick optimization capability provides some new insight into the potential performance of grid-stiffened panels, with specific application shown here to a recent composite grid stiffened design and analysis for the U.S. Air Force Space and Missile Systems Center Orbital/Suborbital Program (OSP) space launch vehicle fairing, Fig. 4. Due to weight and cost goals, a grid-stiffened panel concept is being considered as a redesign of the existing

honeycomb sandwich panel concept. By designing the fairing panels to carry operational loads past the point of linear buckling (local post-buckling), the resulting grid stiffened panel concept is lighter and 30% less costly to manufacture than other design candidates. A structural certification-by-analysis process was implemented by the HyperSizer developers to validate the tools accuracy of predicting the onset of local buckling and the final post-buckling load. In addition to comparing to experimental test data, the validation also included comparisons to the well established STAGS and MSC/NASTRAN FEA tools. Once validated, HyperSizer was used to simulate and optimize all design sizing dimensions and composite material layups of the fairing for local-post buckling operation.



Fig. 4, Orbital's Minotaur OSP space launch vehicle with the existing honeycomb fairing.

1.3 Topics covered in this Paper

By nature of their shapes, grid-stiffened panels are both orthotropic and unsymmetric, even when fabricated with conventional metallic materials. These additional panel behaviors complicate the formulation of stiffness, thermal expansion, and thermal bending. Quantifying these behaviors is important because they significantly alter computed force, moment, curvature, strain, stress, and load carrying capability. The thermoelastic panel formulation shown in the next section quantifies these responses. Also discussed in this section are the failure analyses performed and the optimization approach from a user's perspective. The following section, which is the main portion of the paper outlines the local post buckling method. The effective width approach is shown to be useful for predicting local post buckling behavior. An interesting simulation of the buckling mode progression is illustrated. The test article, failure load results, and pretest analyses are summarized. Lastly, application of local post buckling optimization for the entire fairing design is described.

2. IMPLEMENTATION

2.1 Thermoelastic Formulations

The grid-stiffened panel formulation begins with a review of laminate formulations. For a layered material, the membrane, membrane-bending coupling, and bending stiffnesses are noted as

$$(A_{ij}, B_{ij}, D_{ij}) = \int_{-h/2}^{h/2} (\bar{Q}_{ij})_k (1, -z, z^2) dz \quad (1)$$

Reference [3] shows the corresponding thermal force and moment coefficients to be

$$(A_i^\alpha, B_i^\alpha, D_i^\alpha) = \int_{-h/2}^{h/2} (\bar{\Phi}_i)_k (1, -z, z^2) dz \quad (2)$$

In equation (1),

$$\bar{Q}_{ij} = Q_{ij} [T]^4 \quad (3)$$

are the transformed reduced layered elasticities of the laminae. $[T]^4$ is a fourth order transform tensor and Q_{ij} are, as an example

$$Q_{11} = \frac{E_x}{(1 - \nu_{21}\nu_{12})} \quad (4)$$

In equation (2),

$$\bar{\Phi}_i = Q_{ij} \alpha_i [T]^2 \quad (5)$$

are the transformed reduced layered thermal force coefficients. α_i are the material expansion coefficients. This approach extended to panel concepts has been shown in reference [3] to be

$$(A_{ij}^p, B_{ij}^p, D_{ij}^p) = \int_{-h/2}^{h/2} (\bar{Q}_{ij}^*)_k (1, -z, z^2) dz \quad (6)$$

and

$$(A_i^\alpha, B_i^\alpha, D_i^\alpha) = \int_{-h/2}^{h/2} (\bar{\Phi}_i^*)_k (1, -z, z^2) dz \quad (7)$$

for the panel membrane, membrane-bending coupling, and bending stiffness terms and thermal coefficients. The asterisks indicate laminate and not lamina properties. The laminate properties are defined as

$$\bar{Q}_{ij}^* = \frac{A_{ij}}{t} \quad (8)$$

$$\bar{\Phi}_i^* = \frac{A_i^\alpha}{t} \quad (9)$$

Material properties are interpolated from a database, providing non-linear temperature and load dependent data based on the aircraft trajectory event. The FEA computed tension or compressive load and in-plane and through-the-thickness temperature gradients are used to generate these laminate or metallic sheet properties. If the panel sheets are laminates, the properties of the sheet are treated as being heterogeneous, with actual D_{ij} terms included.

The equivalent plate formulation of any stiffened panel shape, through extension of classical lamination theory, is accomplished by locating a reference plane, identifying its layers with a k_i value, and defining the h_i heights from the reference plane. The panel layers, in this sense, are the facesheet and rib laminates. A reference plane shift is handled by treating a laminate as homogeneous via equations (8 and 9). This approach produces the following general equations for panel stiffness terms and thermal coefficients.

$$(A_{ij}^p, -2B_{ij}^p, 3D_{ij}^p) = \sum_{k=1}^n \frac{h_{k-1}^m - h_k^m}{S_k} (\bar{Q}_{ij}^*)_k \left[\frac{w_k}{C_1} \right] (m = 1, m = 2, m = 3) \quad (10)$$

$$(A_i^{\alpha p}, -2B_i^{\alpha p}, 3D_i^{\alpha p}) = \sum_{k=1}^n \frac{h_{k-1}^m - h_k^m}{S_k} (\bar{\Phi}_i^*)_k \left[\frac{w_k}{C_1} \right] (m = 1, m = 2, m = 3) \quad (11)$$

where for the angle web and the case of

$$ij = 11 \quad C_1 = 2\cos\theta^4$$

$$ij = 22 \quad C_1 = 2\sin\theta^4$$

$$ij = 12, 21, 33 \quad C_1 = 2\cos\theta^2\sin\theta^2$$

S_k is the distance of the repeating pattern of rib spacing (0, 90, or angle) and w is the width, t is the thickness, and θ is the angle of the "angle stiffener" segment. Each stiffness term and thermal coefficient is the summation of all laminate/metallic-sheet segments. In this way, each segment and its direction can be accounted for in any panel concept.

Out-of-plane G_{ij} stiffnesses are included as well as the actual D_{ij} of the laminates. For relatively thick and closely spaced webs, torsional stiffness of the stiffeners are included.

2.2 Failure Analyses

All classical lamination theory loading components are included: N_x , N_y , N_{xy} , M_x , M_y , M_{xy} , and the out-of-plane Q_x and Q_y shears. The loads can come automatically from FEA or be manually input by the user (user defined). In either case, all analyses begin with a balanced FBD with force equilibrium and strain compatibility accuracy checks performed for all panels/beams. If the loads are user defined, any general combination of boundary conditions for thermal and mechanical loading environments can be selected and then the virtual forces and moments are derived for any edge boundary condition or applied force or strain field.

When the grid-stiffened panel concepts are sized, the follow analyses are performed:

Analyze material strength

- Isotropic yield/ultimate stress allowables
- Composite ply-by-ply failure theories: max stress, max strain, Tsai-Hill, Tsai-Wu, Tsai-Hahn, and Hoffman for all laminates of a panel/beam cross section
- Strain/stress fields for all panel locations including bond line joint areas
- Composite unloaded holes and bolt bearing loads

Analyze thermoelastic stiffness effects

- Strain and curvature deformations, and panel and beam midspan deflections for simple and fixed boundary conditions due to pressure
- Panel and local modal frequencies

Analyze panel and beam buckling

- Any longitudinal, transverse, and shear force combination including load interactions
- Unsymmetric, biaxial, membrane-bending panel buckling and bending-twisting coupling effects, and out-of-plane transverse shear flexibility effects
- Ritz energy buckling solutions, cylindrical, multiple boundary conditions

- Buckling-crippling, Johnson-Euler interaction

Analyze local buckling

- All facesheet and rib spans, widths, and thicknesses are automatically identified per design concept
- Boundary conditions are automatically determined, such as free versus simple supports

Analyze crippling

- Isotropic materials for formed and extruded sections
- Composite materials using the D_{ij} bending stiffness terms of the panel and beam laminates as recommended in the recent Mil-Hdbk-17-3E.

2.3 Coupling to FEA

The Mindlin plate form is used to represent the equivalent continuum of grid layout and as a result can be directly incorporated with a FEM. Mathematical coupling to MSC/NASTRAN, I-DEAS, and FEMAP is incorporated. HyperSizer has automated the process of passing data with these solvers and modelers.

2.4 Sizing Optimization

The approach used to effectively analyze any panel concept within the grid-stiffened family, Fig. 5, is to identify analysis objects that make the common set of building units for a panel concept. Each analysis object has particular characteristics. Panel concepts, such as the orthogrid and isogrid share the same analysis objects. Because of the generality of the thermoelastic panel formulations and the assignment of analysis methods to each of the analysis objects, HyperSizer is able to optimize all design options simultaneously.

While in the software interface, the user is able to select the most general of cross sectional dimensions for the panel objects. As shown as a way of illustration in Fig. 6, the user is able to click on different pieces of the panel, and then specify unique sizing optimization bounds to each of the thicknesses, heights, spacings, materials, and layups. The generality also handles all material types, such as aerospace metallics (isotropics), Polymer fiber reinforced composites (orthotropics/layups/laminates), and Hybrid laminates with plies of tape, fabric, metallic sheet, foam, and honeycomb material. To handle manufacturing objectives, the software can also automatically link independent variables, such as the thicknesses or heights of the 0, 90 and/or angle stiffeners. In addition, the software allows linking of design variables across adjacent structural components.

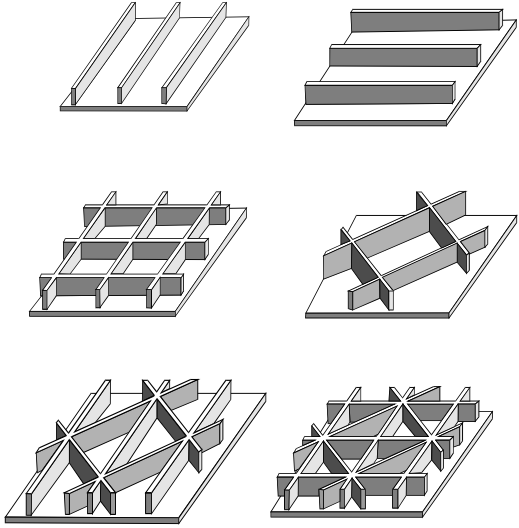


Fig. 5, The user can select any one panel concept from the grid-stiffened family, or any combination to let the optimizer determine the optimum for a given thermomechanical loading.

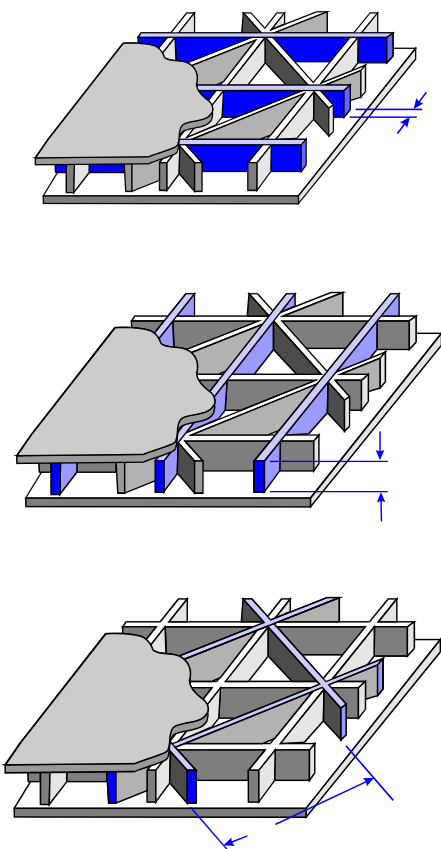


Fig. 6, Each panel facesheet and rib can have independent thicknesses, heights, spacings, materials, and layups, or they can be dependently linked.

3. LOCAL POST BUCKLING

A panel span (usually the facesheet that spans stiffeners) is able to carry additional load after it local buckles due to its remaining effective width. Furthermore, the panel as a whole is also able to carry additional load due to its remaining stable cross section. Local buckling at operating load occurs due to a relatively wide width in comparison to sheet thickness (a high b/t ratio). Such typical aerospace designs are called skin-stringers. Local post buckling of a span is permissible if the panel can be shown to support additional load beyond the first occurrence of buckling (bifurcation point), without strength failure or collapse from buckling or cross section crippling. In aerospace designs, the spans are allowed to local buckle even at limit loads, but normally not at loads below a prescribed level, such as 0.3 DUL.

3.1 Industry Approaches for Calculating Effective Width with Hand Methods

The industry method for calculating effective width for the facesheet of a stiffened panel is to use eqn (12), with crippling stress of the stiffener as the reference stress (crippling stress is noted as F_{cc} or $F_{cr,st}$). See [10, eqn 5.5.2] and [11, eqn 14.2.1].

Reference [11, eqn 11.1.3] most commonly uses this abbreviated form of the equation

$$b_e = t \sqrt{\frac{KE}{F_{cr,st}}} \quad (12)$$

where

$$K = \frac{k\pi^2}{12(1-\nu^2)} = 0.904k, \quad \text{for } \nu = 0.3 \quad (13)$$

Reference [9] uses a similar approach to calculating effective width and includes some terms for orthotropic stiffnesses of the materials.

$$b_e = 3.96t \sqrt{\frac{\sqrt{D_{11}D_{22}} \text{Exc,skin}}{t^3 F_c \text{Exc,stiff}}} \quad (14)$$

For panels that have the same isotropic material for both the skin and stringer, this equation reduces to

$$b_e = 3.96 \sqrt{\frac{D_{11}}{t F_c}} \quad (15)$$

For isotropic materials, eqn (15) should produce the same result as eqn (12). However, comparing eqn (15) to eqn (12) there is a difference of $6.28/3.96 = 1.586$. We assume this difference is due to a typo mistake in reference [9], which is a preliminary document. Both methods use only the stiffener cross section for computing crippling stress. Neither method attempts to include the effective width of the facesheet for crippling. The method in [9] accounts for crippling-buckling Johnson Euler effects and includes the effective width in the column buckling moment of inertia/radius of gyration properties. [11, Fig 14.2.3] accounts for simple vs. fixed boundary conditions based on the skin b/t ratio.

3.2 A New Approach for Computing Effective Width and Local Post Buckling of Stiffened Panels

The approach for analyzing local post buckling of stiffened panels presented here is to load the panel cross section and determine which, if any, span objects local buckle. A span object could be a stiffener web, a stiffener flange, or a portion of the facesheet. For aerospace applications, it is customary to allow the facesheet between the stiffeners of a skin-stringer design to local buckle at a load below the overall design-to load. The stiffener, as a strip-column, is designed to carry the additional compressive and overall bending moments of the panel. The unbuckled portion of the skin that has an effective width is included in the stiffener's cross section properties.

As an example, lets look at a metallic Zee stiffened panel, Fig. 7a and 7b, that is loaded in uniform compression, or more accurately described by an applied uniform end shortening. At the onset of skin buckling (local buckling) the analysis is linear elastic, and all of the panel objects such as the skin, stiffener web, and stiffener flange are all at the same stress level. This level of stress is depicted as the horizontal dashed line in figure 7c. As applied load is added to the panel, the buckled skin between stiffeners remains at the same stress (constant bifurcation load) and the additional load is picked up by the stiffener and the remaining effective width, b_e of the skin. As more load is applied the effective width becomes more narrow and the remaining stable cross section of skin and stringer carries a higher stress, until either the material reaches compressive yield, the strip-column buckles, or the stiffener cripples. An actual state of stress distribution of Fig 7d is represented with rectangular areas, Fig. 7e.

Therefore we observe the effective width is a function of the referenced stress, σ . For stiffened cross sections hand methods use for this referenced σ , either the limiting allowable crippling stress of the stringer, $F_{c,st}$, a buckling-crippling interaction stress such as Johnson-

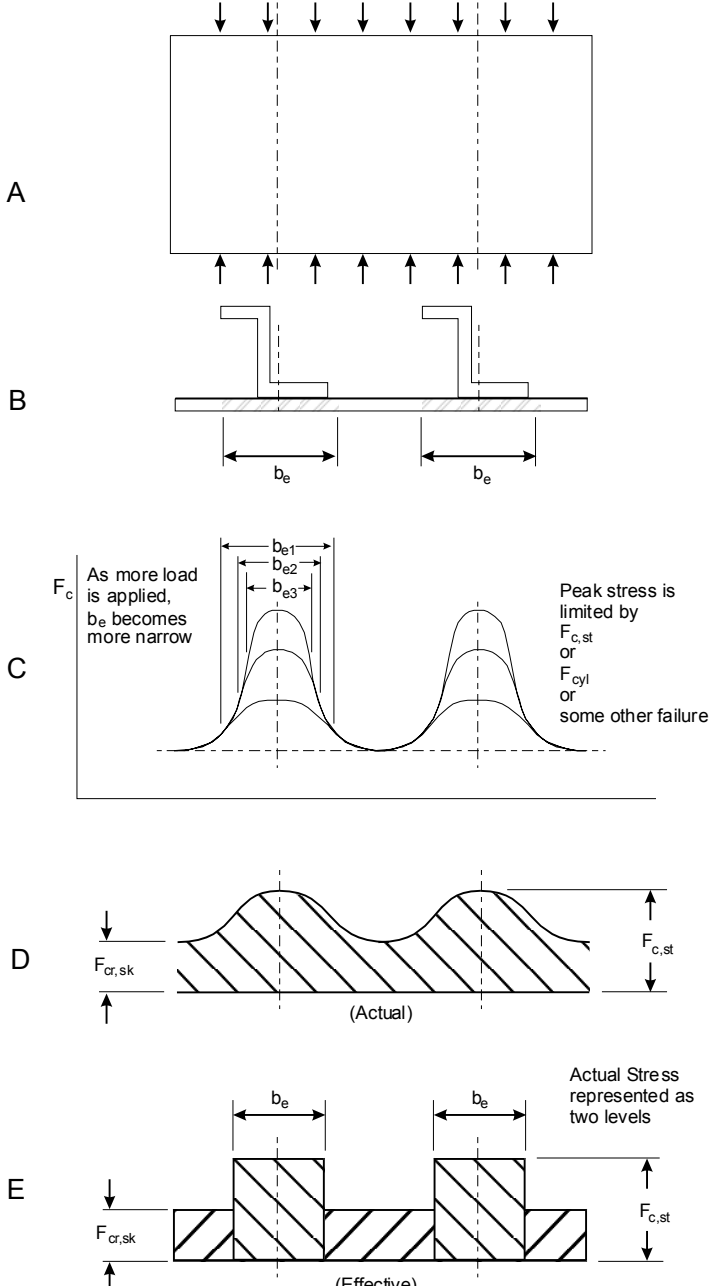


Fig. 7, The effective width of the facesheet is included with the stiffener in the calculation of remaining panel stable cross section. As load is increased the remaining effective width becomes more narrow.

Euler, F_c , or the compressive yield stress of the material, F_{cyl} . HyperSizer uses for the reference stress, the actual state of stress in the panel objects for each loadcase, and as an internal check, verifies that the convergence of inelastic stresses times their corresponding widths integrates to the applied loading.

3.3 HyperSizer General Method to Local Post Buckling and Effective Width

HyperSizer incorporates all of the effects as captured with the hand methods, but does so in a more general and robust manner. A more general approach permits more loadings and structural responses to be included. Some primary benefits are listed here.

- Not only are compressive axial loads used, but also biaxial loadings, including tension field hoop effects, shear loadings, and bending moments including beam-column. (For instance, effective widths are computed for a facesheet in compression caused from bending moments)
- Full support for composite orthotropic materials
- Redistributions load for the change in remaining stable cross section and converges the solution
- Removes the bifurcation load of the buckled skin from the remaining stable cross section
- The corresponding redistribution of internal loads are used by all of the failure analyses such as material strength, panel buckling, crippling, etc.
- The reference σ used for calculating the effective width is the actual σ in the panel objects and not a worst case allowable reference σ
- Applicable to other stiffened objects such as the web or flange, and not fundamentally limited to a facesheet
- Can specify that local buckling is to never occur below % of Design Limit Load (such as 45% DLL)
- The post buckling option causes only a slight increase in optimization run times, its implementation is very efficient

3.4 HyperSizer Specific Implementation to Local Post Buckling and Effective Width

The HyperSizer specific implementation is best introduced with a flowchart, Fig. 8. Here we see how local post buckling is incorporated into the program logic. Note that there are two major convergences. The first convergence is noted with the blue dashed box and is for the effective width. This convergence is performed on an inner program data flow level, while the second convergence is for the overall panel stiffness and internal load redistribution, which occurs on an outer program logic level.

Converge effective width The process begins by performing a typical linear elastic analysis and identifying a panel object that has local buckled, such as the facesheet/skin between stiffeners. The full unit load of N_x , N_y , and N_{xy} in that object, per loadcase, is then used with an orthotropic mode shape minimization buckling routine to iterate on the sheet width, to cause it to be just at the point of buckling bifurcation. Once converged, this is noted as the effective width. In other

words, the effective width is capable of supporting the N_x , N_y , and N_{xy} loads without buckling. This process is in contrast to a hand method which uses eqn (12) or (14) to directly compute the effective width.

Converge the overall panel stiffness: Once the effective width of an object is determined, then the remaining stable cross section can be determined for computing new generalized stiffness matrices [A], [B], and [D], including corresponding thermal coefficients for membrane, bending, and membrane-bending coupling. These updated stiffnesses and thermal coefficients will cause an update in forces of all objects, which cause a change in the reference stress and a change in effective widths. Also additional objects might local buckle. This cycle is repeated until convergence.

Subtract the local buckled objects bifurcation loads from the overall panel: The N_x , N_y , and N_{xy} unit forces in the object at onset of local buckling are identified, Figure 7.c. These forces will remain constant as other parts of the panel are able to support more load. These forces are multiplied by the ineffective width of the object (the width already buckled, not part of the stable cross section) and subtracted from the panel applied loads.

Note that the effective width convergence and update of stiffness is performed for any combination of loading that causes a span object to local buckle. Also note that the update stiffness for the remaining stable cross section, with its corresponding redistribution of internal loads into the unbuckled objects, is used by all analyses such as panel buckling, beam-column buckling, crippling, frequency, deformation, material strength, etc.

Verify that all analysis objects are getting the correct values of 3-D transformed laminate strain fields. Each analysis object's strain field is computed by transforming the panel's reference plane strains and curvatures into each analysis object's local coordinate system. These strains are then transformed again into ply-by-ply strains. By using each ply's constitutive properties, a ply-by-ply stress field is integrated to determine the laminate force and moment components in each object's local coordinate system. These force and moment contributions are then transformed again into the panel coordinates to verify that their weighted summations equal the applied panel external loadings. Therefore Free Body Diagram (FBD) force equilibrium and strain compatibility are ensured throughout the process of converging both the effective width and overall panel stiffness.

Analysis Process - Local Post Buckling

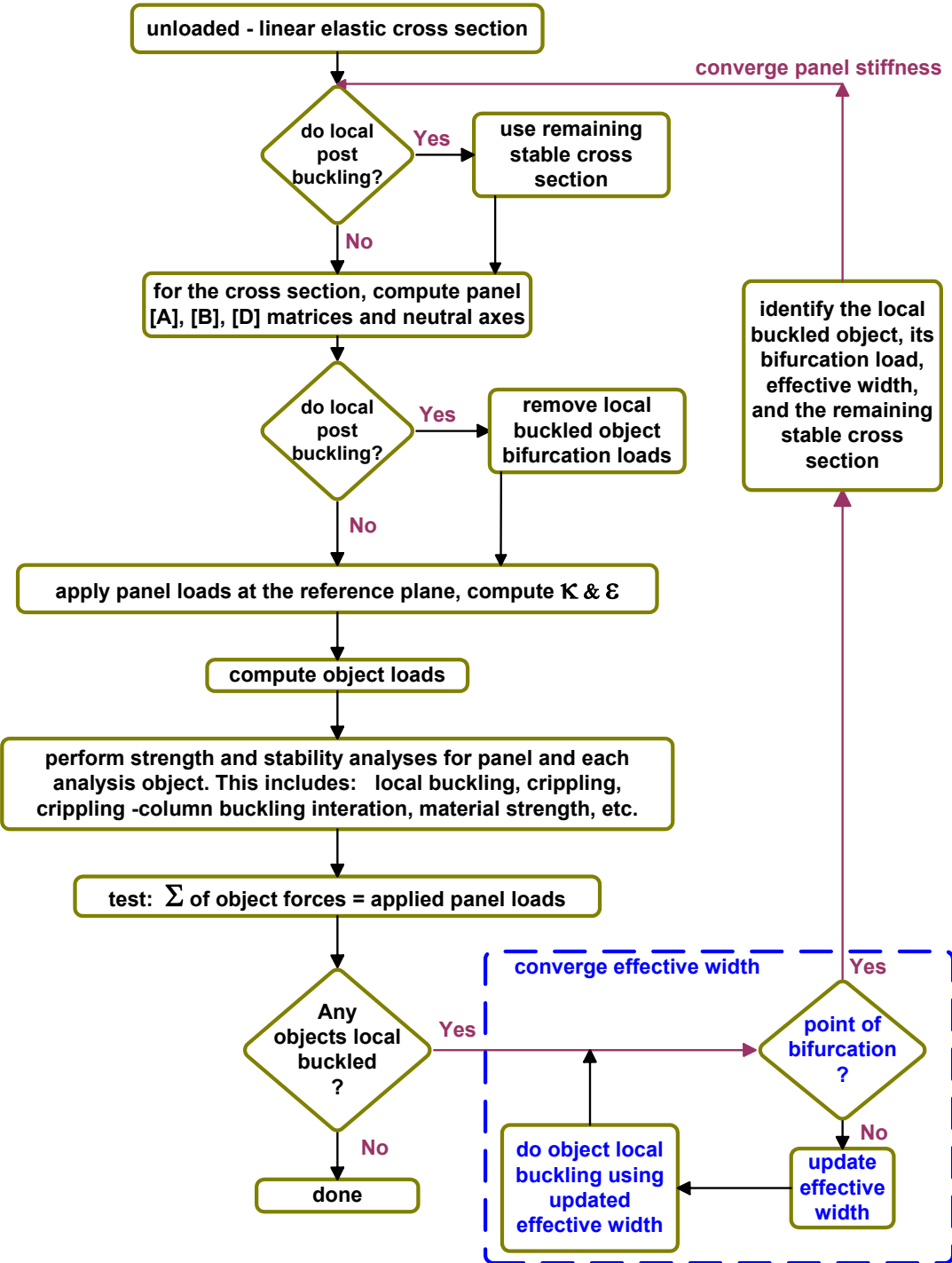


Fig. 8, The overall analysis method for converging the effective width and panel stiffness as the local post buckling progresses. This process is implemented in HyperSizer and was used for predicting the grid stiffened panel test failure load.

4. EXPERIMENTAL TEST SETUP

4.1 Material Properties: IM7/8552 tow

Ply t (in) = 0.00575,	ρ (lb/in ³) = 0.057
E11t (msi) = 20.6,	E11c (msi) = 18.28
E22t (msi) = 1.43,	E22c (msi) = 1.56
G12 (msi) = 0.66,	ν_{12} = 0.31
Ftu11, 0° (ksi) = 338.11,	Fcu11, 0° (ksi) = 224.83
Ftu22, 90° (ksi) = 13.82,	Fcu22, 90° (ksi) = 37.76
Fsu12 (ksi) = 15.18	

4.2 Layups

Facesheet = 8 ply [90/20/0/-20/-20/0/20/90]

Average laminate thickness = 0.046"

0° Rib Stiffeners = all (0) plies

Average laminate thickness = 0.184"

90° Rib Stiffeners = all (0) plies

Average laminate thickness = 0.124"

4.3 Panel Dimensions

Length = 44.75", Width = 32.08"

Radius of Curvature = 30.42"

0° Rib stiffener spacing = 8.02"

Angle Rib stiffener spacing = 13.77", Angle = 35.63°

Rib heights = 0.72", Total height = 0.766"

4.4 Loading

The axial compression was applied as a uniform end shortening. Even though the load is uniaxial compression on the panel edge, due to the angle ribs, a biaxial force develops in the facesheets.

4.5 Boundary Conditions

Fixed at both ends. Free on the sides with a point constraint at the edge midspan.

5. SIMULATION OF INCREASED LOADING TO POST BUCKLING FAILURE

5.1 Transition from local buckling of the skin to buckling collapse of the panel

Fig. 11 shows a progression of the local buckling mode shapes of the skin pockets upon increased loading. The buckling images on the left are those predicted with MSC/NASTRAN geometric non-linear analysis. The images on the right are measured experimentally. By inspection of the rib diagonals, one can determine that the measured graphic is of a smaller area of the panel center, whereas the FEA model is of the entire test panel. Keeping this in mind, fairly close comparison between the pattern of out-of-plane displacements is observed. Fig. 13b better portrays the measured out-of-plane displacement.



Fig. 9, Grid stiffened test panel in loading cell.

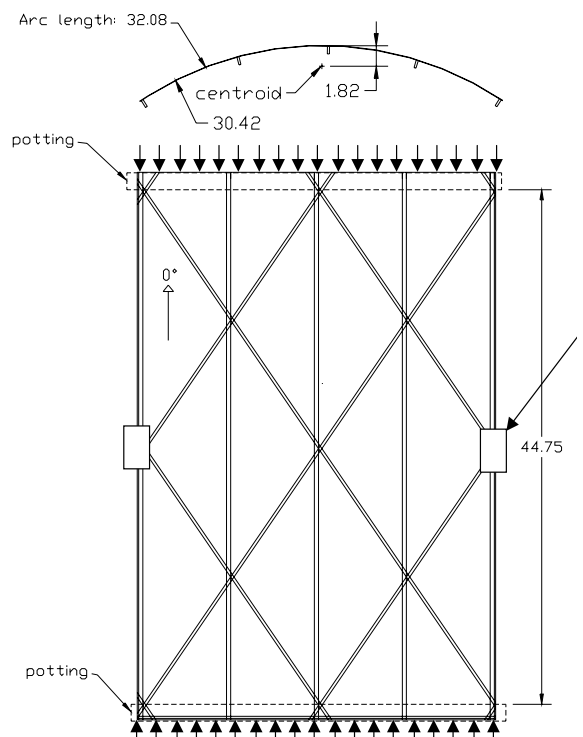
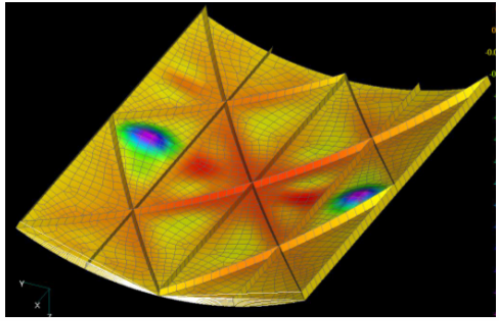


Fig. 10, Schematic of Grid stiffened test panel.



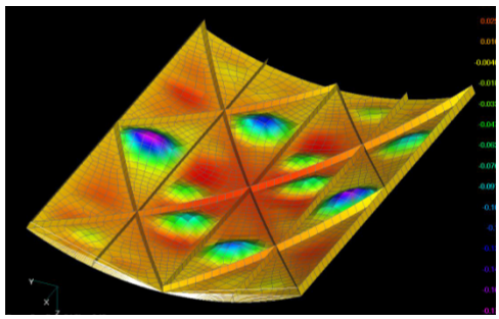
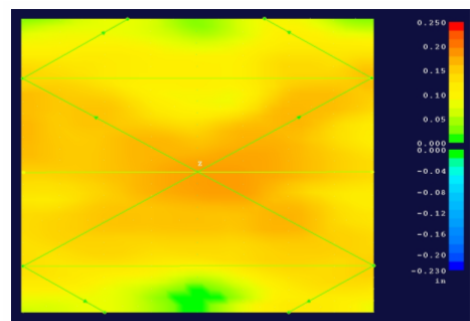
Initial Local Buckling

235, Test result

265, HyperSizer

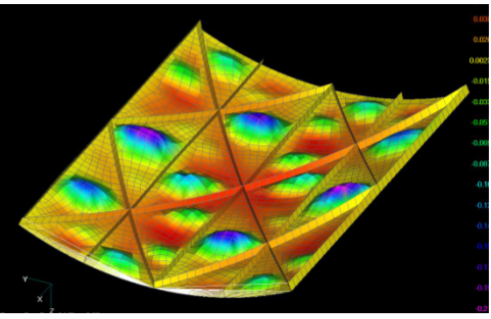
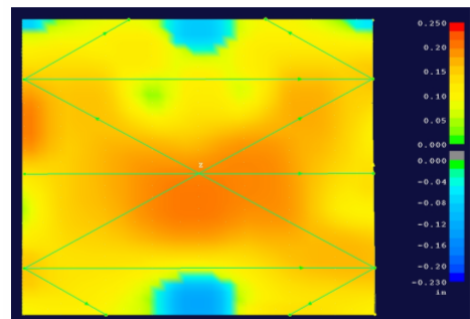
310, STAGS

340, MSC/NASTRAN



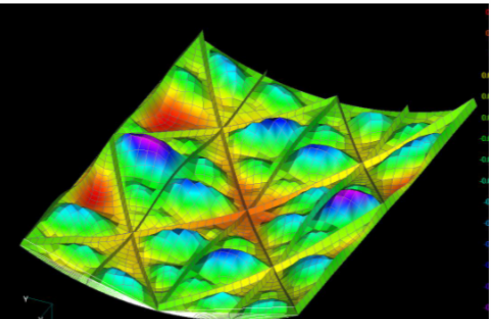
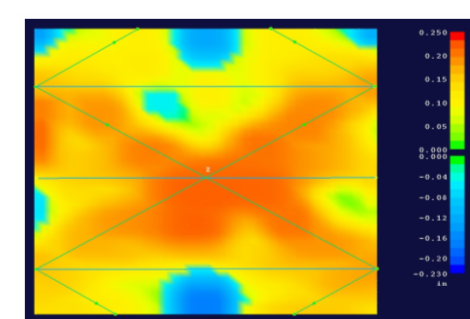
An Intermediate Stage

470



An Intermediate Stage

780



Post-buckling panel collapse

1320, Test result

1300, HyperSizer

1250, STAGS

1425-2000, MSC/NASTRAN

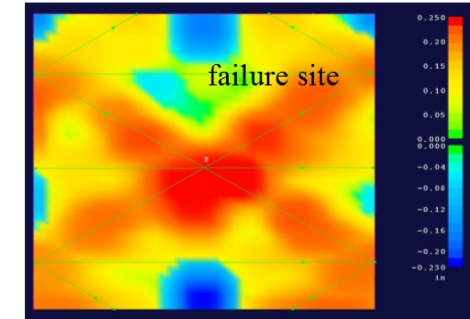


Fig. 11, Simulation of the buckling mode shapes as load is increased on the panel. All loading values are reported as unit loads (lb/in). The images portray out-of-plane displacements. The left images are those produced with MSC/NASTRAN non-linear geometric analysis. The images on the right are the measured experimental values.

5.2 Simulation of Effective Width of Unbuckled Facesheet

The left images of Fig. 12 are the NASTRAN FEA geometric nonlinear solutions of out of plane displacements (T3) for a given load increment. The corresponding right image is the plot of the FEA computed nonlinear Nx load as imported into HyperSizer. Note how the pocket,

local buckling causes the Nx load to distribute in bands, where the value of Nx in the path of a buckle is reduced, as additional load concentrates in the unbuckled skin widths over top of the rib stiffeners. As the overall panel Nx load is increased, the unbuckled effective widths become fully developed, as indicated by the gray hashed lines.

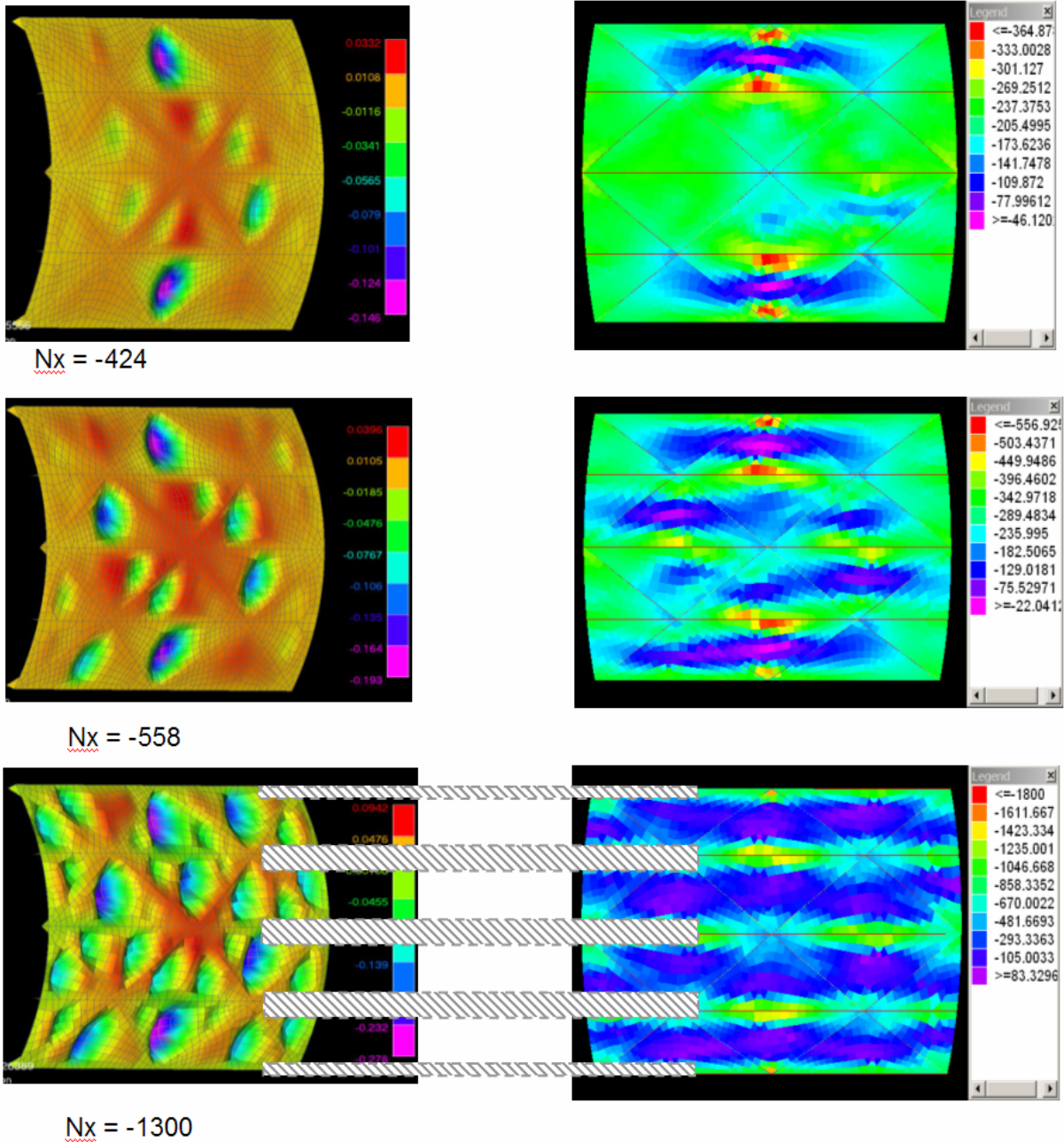


Fig. 12, Simulation of the buckling effective width. The facesheet side is shown with ribs hidden. As more load is applied, a clear distinction is observed between buckled skin and unbuckled skin effective width as indicated with the horizontal bands. As post buckling collapse is reached, the effective widths are fully developed and become quite narrow.

5.3 Failure Load and Mode

Skin pocket buckling occurred from 220 to 250 (lb/in) gradually with some instances of oil-canning.

Panel collapse occurred at 1320 (lb/in). Investigation of the test article after collapse indicates failure consisted of delamination and buckling in axial and diagonal ribs and skin, and axial rib compression/shear fracture.

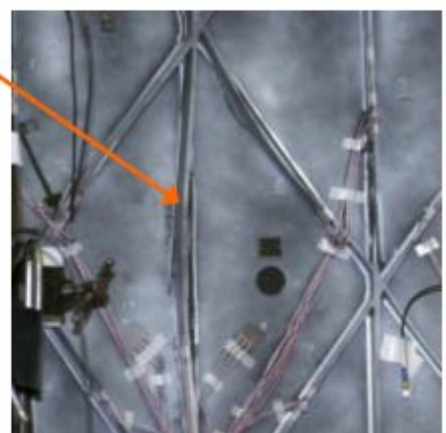
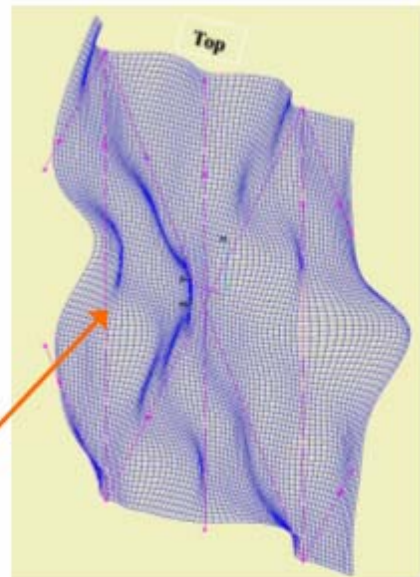
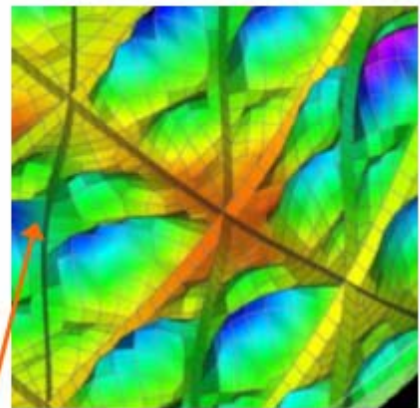
HyperSizer predicted panel collapse at 1300 (lb/in) due to column buckling of the 0-degree (longitudinal) rib. Experimental data from Figs 13b and 13c, and the FEM displacement plot, Fig 13a, appear to corroborate this finding.

At the point of failure, it is interesting to see that all of the post buckling analyses (MSC/NASTAN, STAGS, and HyperSizer) show multiple half wave buckling modes in the facesheet pocket which compares well to the observed experimental response, Fig 13b. Maximum measured out-of-plane displacement of the skin pockets was 0.22 inches.

Fig. 13, Close up views of the failure location.

- a) Top image, computed deflection at 1245 (lb/in) compression load.
- b) Middle image, 10 x measured deflection at 1250 (lb/in) compression load.
- c) Bottom image, damage to panel after failure.

Final failure appears to be caused by buckling instability of the longitudinal, 0°, rib in column buckling.



6. SUMMARY OF PRETEST ANALYSIS PREDICTIONS COMPARED TO EXPERIMENTAL TEST RESULTS

SUMMARY TABLE: PRETEST FAILURE ANALYSES

Method	-Nx (lb/in)
<i>Linear elastic buckling (local pocket buckling)</i>	
• Test Data	235
• HyperSizer FBD linear ¹ (<i>including a 0.9 knockdown factor</i>)	265
• NASTRAN eigenvalue (<i>including a 0.8 knockdown factor</i>)	345
• NASTRAN geometric non-linear analysis	340
• STAGS, eigenvalue (<i>including a 0.8 knockdown factor</i>)	310
• STAGS, non-linear analysis	310
<i>Non-linear/post buckling² (panel buckling and/or crippling)</i>	
• Test Data	1320
• HyperSizer FBD nonlinear ³ (<i>including a 0.8 knockdown factor</i>)	1300
• NASTRAN ⁴ , geometric non-linear, <u>practical post buckling load limit</u> using HyperSizer for material strength and crippling ⁵	1425
• NASTRAN ⁴ , geometric non-linear, <u>theoretical limit</u> based on solution non-convergence, and falling load carrying capability	2000
• STAGS ^{4,6}	1250

In general practice; a ***knockdown factor*** is applied to linear buckling solutions to account for imperfections. This is because linear buckling solutions are not sensitive to imperfections. The long-established 0.8 factor is used in our linear FEA analyses and HyperSizer panel buckling. A 0.9 is used for HyperSizer local buckling analyses. Geometric non-linear solutions are sensitive to imperfections and in general practice a knockdown is not applied to their buckling predictions.

¹ The authors do not imply HyperSizer is better than FEA for predicting onset of local buckling of the

triangle pocket. These were pretest predictions of just one single test.

² The panel exhibits considerable, analytically predicted additional post buckling load carrying capability. In order to achieve these relatively high levels of post buckling strengths, debonding/delamination must not occur between the stiffeners and facesheet. Delamination pretest analyses were not performed. If stiffener separation doesn't occur, these are the potential post buckling failure loads.

³ For the nonlinear analysis performed, only the HyperSizer solutions considered the material strength and crippling post buckling failure modes. HyperSizer solutions were very quickly obtained using its Free Body Diagram (FBD) loading option. A knockdown factor still applies to HyperSizer post buckling since its effective width approach is not a full fledged geometric nonlinear solution that would pick up imperfections.

⁴ The geometric nonlinear MSC/NASTRAN FEA and STAGS solutions may not be as accurate as possible because only one finite element was used to represent the depth of the stiffening ribs. The same FEM mesh was used by both codes. Based upon the final post buckling analyses of both FEA codes, it appears STAGS better handled the coarse model.

⁵ The practical MSC/NASTRAN FEA cutoff limit was determined by importing into HyperSizer the non-linear FEA computed post buckled forces and moments of the laminates. HyperSizer performed material strength and crippling analyses for the laminates for each of the load increments. HyperSizer identified the load increment that would cause a fiber failure or facesheet-stiffener cross section crippling. Using a 5500 μ in/in max strain limit, several panel bays failed in material strength at Nx = -1425. A 5500 strain limit is a commonly used composite strength design allowable for providing damage tolerance. The actual material strength of this test article is likely higher than 5500. However, since delamination/debonding pretest analyses were not performed, 5500 seemed to be a proper strain allowable.

⁶ The STAGS solution was showing a post buckling transition and non-convergence at this load. Some attempts were made to continue the solution beyond Nx=-1250, however the analysis was stopped there, with the belief that panel collapse was reached.

7. COMPLETE FAIRING STRUCTURAL ANALYSIS AND OPTIMIZATION

After establishing analysis method verification, a grid stiffened fairing is being designed with HyperSizer for the Minotaur launch vehicle. It will be larger in diameter and replace the existing cylindrical shaped honeycomb fairing used today, Fig. 14.

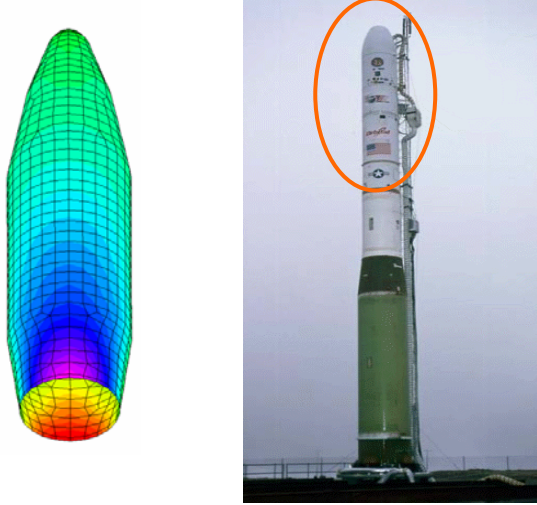


Fig. 14, Left image is a coarse meshed 2D planar FEM in the shape of the new larger diameter fairing that is to replace the existing fairing.

Since the experimental test article is statically determinate, the overall loads in the panel were known without the need for FEA. For the test article, the edge compression load, or alternatively the uniform end shortening, was entered directly into HyperSizer along with appropriate boundary conditions. Conversely, the dynamic flight pressures on the fairing surface require FEA to resolve internal loads. Accordingly for the fairing design, the finite element loads from a coarse meshed FEM, Fig 14, are automatically imported into HyperSizer for analysis and optimization (referred to as sizing). Since HyperSizer contains all information about the grid design such as panel concept, rib spacing, height, layups, thicknesses, and ply material properties, it generates fully defined stiffness terms for the FEM in a 2D planar equivalent form. Therefore a single plane of shell elements, such as NASTRAN CQUAD4 can be used by a coarse meshed model to represent both the facesheet and ribs of a stiffened panel [3].

7.1 The Need for a Tool like HyperSizer

In a design situation, without a tool like HyperSizer, industry would perform the many analyses for each load condition by hand or with a spreadsheet and iterate

based on intuition until a satisfactory design was found. Then a FEM would be built to verify the design. General purpose FEA codes provide the accuracy but require considerable effort in generating a surface FEM mesh that includes discrete modeling of the stiffened cross section. Furthermore, once made, the FEM is only suitable for a given cross sectional shape and size. If the original design is not capable of supporting the intended loads, or if many different concepts and sizes are to be considered (i.e. optimization), than many more FEM meshes need to be generated. In contrast to being locked into a single grid stiffened design, the HyperSizer analysis method obtains relatively accurate solutions using a 2D planar approach for the FEM reducing the need to always model a stiffener's shape, size, and spacing.

7.2 Global – Local Post Buckling Sizing

HyperSizer is a local sizing tool that performs analyses on the panel level such as panel buckling, crippling of the cross section, and local buckling of the individual facesheet spans and ribs. As the remaining effective stiffness of the panel cross section is continually reduced as post buckling of the facesheet advances to higher loads and less effective width, all local failure analyses are repeatedly performed during the optimization. Once it has found an optimum panel or beam design it updates the FEM. At that point it may be necessary to run a buckling solution for the entire system to capture potential global buckling modes. When the designs are linear elastic (i.e. no post buckling allowed), these iterations between HyperSizer and FEA need only be performed for each design update cycle. However, nonlinear post buckling iteration coupling between the local and global may need to be performed at intermediate load steps. In the case of this fairing design, such is not the case in that a check of the final post buckled panel properties did not cause global buckling to be critical. Panel buckling remained critical, and the FEM needed to be updated only once.

7.3 Fairing Design, Post Local Buckling Verification

Once an optimum design is found, the buckling loads and modes as predicted with HyperSizer were compared between the linear elastic solutions and the post buckling solutions. As expected, the panel buckling loads were less and the buckling mode shapes became different as the panel stiffnesses were reduced due to post buckling.

Shown in Fig. 15 is the buckling mode of the complete launch vehicle fairing as computed with a 2-D equivalent FEM mesh using MSC/NASTRAN with HyperSizer updated, local post buckling grid stiffened panel stiffness properties. As a further validation, the

HyperSizer post buckling predictions match panel for panel these global modes predicted with FEA, Fig. 15.

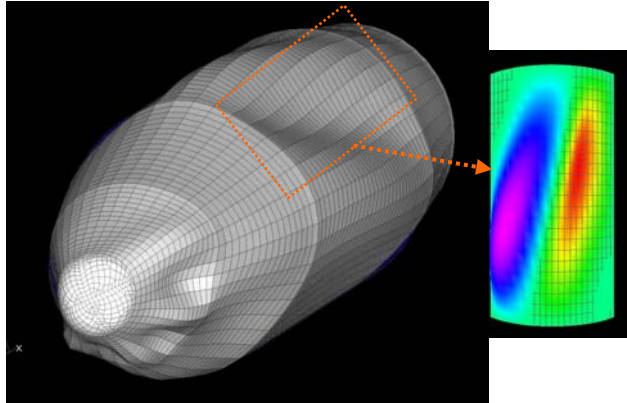


Fig. 15, Verification of the global post buckling response of the final optimum grid stiffened, cylindrical shaped fairing design. Solution on the left is NASTRAN FEA buckling of the fairing. The orange box outlines the same area analyzed with HyperSizer buckling, on right. The post-buckled stiffness properties were used by both tools producing the same buckling load and mode shape.

8. CONCLUSIONS

- 1) HyperSizer was reliably accurate at predicting the onset of local buckling and final post buckling collapse of this grid stiffened test article.
- 2) The unique capability provided by HyperSizer is its design sizing for finding an optimum gird stiffening pattern, depth, spacing, rib angles, and facesheet and rib layups.
- 3) The statically determinate test article's compression load, with choice of boundary conditions, was entered directly into HyperSizer without the need for FEA. For the launch vehicle fairing design, FEA is required for computing the internal loads. Once computed, the loads were imported into HyperSizer automatically. Regardless of how the loads get into HyperSizer, the same analyses and sizing optimization is performed.
- 4) Some HyperSizer deterministic local analyses may be considered high fidelity, while others are between low and high fidelity. Future development is directed towards achieving reliable accuracy by implementing probabilistic methods grounded with test data.

9. ACKNOWLEDGMENTS

Design, fabrication, testing, and data acquisition of the composite, grid-stiffened test article panel was

performed by the Boeing Company in Seattle, WA on 12 June 01. **Barry Van West** is the Boeing project manager and technical lead. The test article analyses presented herein supports certification of a new grid-stiffened fairing design for OSC's Minotaur launch vehicle, an operational Air Force system. The work performed by Boeing, and the optimization trade studies performed by Collier Research were funded by the Air Force Research Lab. **Dr. Peter Wegner** of the Air Force Research Lab, Kirtland AFB, NM, manages this project and provides overall vision and technical direction.

The STAGS solutions were performed by **Rick Young** of NASA Langley Research Center. The authors thank Rick and NASA for their support.

10. REFERENCES

1. *Isogrid Design Handbook* - McDonnell Douglas, NASA CR-124075, Rev. A, Feb. 1973
2. Huybrechts, S. "Advanced Grid Stiffened Composite Structures" Air Force Research Lab, Space Vehicles Directorate, May 25, 1998.
<http://composite.about.com/business/composite/library/weekly/aa980525.htm>
3. Collier, C.S., "Thermoelastic Formulation of Stiffened, Unsymmetric Composite Panels for Finite Element Analysis of High Speed Aircraft", 35th AIAA/ASME/ASCE/AHS/ACS Structures, Dynamics, & Materials Conference, Hilton Head, SC, April 18-20, 1994, AIAA paper 94-1579
4. HyperSizer User's Manual, [Book 2: Analytical Method and Verification Examples](#), Collier Research & Development Corp., Hampton, VA, September 1998
5. Collier, C.S., Yarrington, P.W. and Pickenheim, M.R. "The HyperSizing Method for Structures", NAFEMS World Congress '99 on Effective Engineering Analysis. Newport, Rhode Island, April 25-28 1999, page 853
6. Von Karman, Tl, Sechler, E. E., and Donnell, L. H., "The Strength of Thin Plates in Compression," ASME Transactions, APM-54-5, Vol. 54, No. 2, 30 Jan 1932, pp. 53-57
7. Hilburger, M. W., Nemeth, M. P., and Starnes, Jr., J. H., "Effective Widths of Compression-Loaded Plates with a Cutout", NASA TP-2000-210538, Oct 2000.
8. Young, R. D., Hyer M. W, and Starnes, J.H., "Prebuckling and Postbuckling Response of Tailored

Composite Stiffened Panels with Axial-Shear Coupling”, 41st AIAA/ASME/ASCE/AHS/ACS Structures, Dynamics, & Materials Conference, Atlanta, GA, April 3-6, 2000, AIAA paper 00-1459

9. HSR, High-Speed Research Program Preliminary Analysis/Sizing Handbook for Fuselage Structures, Revision B, 30 Sept 98, pp 30-32

10. Niu, Michael C. Y., *Airframe Structural Design*, 1988, Commilit Press LTD, ISBN 962-7128-04-X

11. Niu, Michael C. Y., *Airframe Stress Analysis and Sizing*, 1997, Commilit Press LTD, ISBN 962-7128-07-4

11. TRADEMARKS

HyperSizer® is a registered trademark of Collier Research Corporation

NASTRAN® is a registered trademark of NASA

MSC/NASTRAN™ is an enhanced proprietary product of the MacNeal-Schwendler Corporation.

STAGS™ is a trademark of NASA